

Volume of 4-polytopes from bivectors

Benjamin Bahr¹

¹ II Institute for Theoretical Physics
University of Hamburg
Luruper Chaussee 149
22761 Hamburg, Germany

Abstract

In this article we prove a formula for the volume of 4-dimensional polytopes, in terms of their face bivectors, and the crossings within their boundary graph. This proves that the volume is an invariant of bivector-coloured graphs in S^3 .

1 Introduction

Loop Quantum Gravity and Spin Foam Models aim at a quantization of General Relativity, using discrete structures. [1, 2, 3, 4]¹ In particular Spin Foam Models rest on the equivalence of GR with constrained BF theory [8, 9, 10]. While the quantization of BF -theory is straightforward [11], the connection to GR is implied by enforcing a version of the so-called simplicity constraints on the quantum theory.

The discrete variables are parallel transport holonomies $g_\ell \in \text{Spin}(4)$ associated to $1d$ curves ℓ , and bivectors $B_f \in \mathbb{R}^4 \wedge \mathbb{R}^4$ associated to $2d$ surfaces f . These latter ones act as derivative operators on the boundary Hilbert space, and the asymptotic limit of the quantum amplitudes can describe transitions in Regge geometry of $4d$ polyhedra P with given classical bivectors B_f associated to their $2d$ subfaces [12, 13, 14].

Also the (discrete, classical version of the) simplicity constraints can be formulated in terms of the B_f , and they can be regarded as conditions to allow a reconstruction of P for given bivectors B_f . In that case the dynamics of the theory is intricately connected to the $4d$ geometry of space-time.

For the special case of a 4-simplex, this reconstruction is known, and the corresponding simplicity constraints have been the foundation for modern spin foam models [15, 16, 17, 18, 19]. While the formula can be extended to arbitrary polyhedra [20], it still rests on the reconstruction of the 4-simplex, rather than that of the respective

¹They share this feature with other, related approaches to quantum gravity [5, 6, 7]

polyhedron (which in general is unknown). In particular, it could be shown that in the case of certain transitions, the corresponding model is underconstrained, and contains additional, non-geometric degrees of freedom. These can be directly traced to an insufficient implementation of the so-called quadratic volume simplicity constraint [21, 22, 23].²

An implementation of this constraint for the special case has been presented in [22], and shown to reduce the system to the correct numbers of degrees of freedom. This constraint rests on a formula for the 4-volume of P in terms of its bivectors B_f . In this article, we will give a proof of this formula for the case of general P . It rests, beyond the bivectors B_f , on the knotting class of the boundary graph Γ of P . In particular, for Γ projected onto the plane with crossings C , the volume V_P of a (convex) polytope P can be expressed as

$$V_P = \frac{1}{6} \sum_C \sigma(C) * (B_1 \wedge B_2), \quad (1.1)$$

where $\sigma(C)$ is the sign of the crossing, B_1, B_2 are the bivectors associated to the graph links involved in the crossing (which correspond to $2d$ faces in a prospective P), and $*$ is the Hodge dual. This formula was also used in [27, 28] to add a cosmological-constant-like deformation to the Spin Foam Model³. In the following, we will prove the formula for general convex polytopes in $4d$.

The strategy of the proof is as follows: First we define an invariant $I(\Gamma)$, as the rhs of (1.1), for arbitrary graphs Γ , hence for arbitrary convex polytopes. Then we show that, when a polytope is cut into two smaller convex polytopes by a hyperplane, the sum of the invariants of the new polytopes add up to the invariant of the old one. Then, we show that in case of a 4-simplex, the value of the invariant coincides precisely with its 4-volume, i.e. (1.1) is true for 4-simplices. Lastly, we show that every polyhedron can be successively cut by hyperplanes, until only 4-simplices remain. This proves (1.1) for arbitrary convex polytopes.

2 Bivector-coloured graphs

Definition 2.1. *Let Γ be a directed graph embedded in S^3 . Denote the set of nodes and (oriented) links of Γ by $N(\Gamma)$ and $L(\Gamma)$. We call a bivector-colouring of Γ a map*

$$B : L(\Gamma) \rightarrow \mathbb{R}^4 \wedge \mathbb{R}^4. \quad (2.1)$$

²Although non-geometric geometries manifest themselves in face-non-matching, they go beyond the so-called “twisted geometries”, which are already present in the 4-simplex case [24, 25, 26].

³The 4-simplex-version of this operator was defined in [29] and used in [30] to define a relation to Chern-Simons theory of a deformed amplitude. A different but related way to include a cosmological constant in the amplitude is by replacing classical with quantum groups [31, 32], which can also be done on the boundary Hilbert space level [33].

If the link ℓ meets the node n , we write $\ell \supset n$. For $\ell \supset n$, we write $[n, \ell] = 1$, if the link ℓ is incoming but not outgoing, -1 if it is outgoing but not incoming, and 0 if it is both or neither. We call a bivector-colouring of Γ simple, if the B_ℓ , for $\ell \in L(\Gamma)$, satisfy the following conditions:

- For ℓ, ℓ' both meeting at n , we have

$$B_\ell \wedge B_{\ell'} = 0. \quad (2.2)$$

Note that this includes the case $\ell = \ell'$.

- For every node in Γ we have that

$$\sum_{\ell \supset n} [n, \ell] B_\ell = 0. \quad (2.3)$$

In the spin foam literature, conditions (2.2) are called “diagonal simplicity” for $\ell = \ell'$ and “cross-simplicity” for $\ell \neq \ell'$, while (2.3) is called the “closure condition”. In the following, we denote, for simplicity, a simple bivector-coloured graph as Γ , rather than $(\Gamma, \{B_\ell\}_{\ell \in L(\Gamma)})$.

We call a projection of Γ onto the plane a representation as graph $\tilde{\Gamma}$ on \mathbb{R}^2 with crossings. A projection can be achieved by choosing a point $p \in S^3$ which does not lie on Γ , then making a stereographic projection $\phi : S^3 \setminus \{p\} \rightarrow \mathbb{R}^3$ w.r.t. that point, to obtain a graph $\phi(\Gamma)$ in a compact subset of \mathbb{R}^3 . A projection is then achieved into some direction such that no nodes lie on top of links, and links only cross one another finitely many times. Any two projections of Γ can be obtained by the following moves on $\tilde{\Gamma}$ [34, 35, 36]:

1. Remove writhing: figure 1.
2. Link sliding over/under links: figure 2.
3. Link sliding over/under crossings: figure 3.
4. Links twisting at nodes: figure 4.
5. Link sliding over/under nodes: figure 5.

Definition 2.2. Let Γ be a simple bivector-coloured graph. For a projection $\tilde{\Gamma}$, there are two types of crossings, depending on the relation of link orientations and over-/undercrossings. These are depicted in figure 6. For a crossing C , define $\sigma(C) = \pm 1$ depending on which of the two cases are present. Then we define the number

$$I(\Gamma) := \frac{1}{6} \sum_C \sigma(C) * (B_{\ell_1} \wedge B_{\ell_2}). \quad (2.4)$$

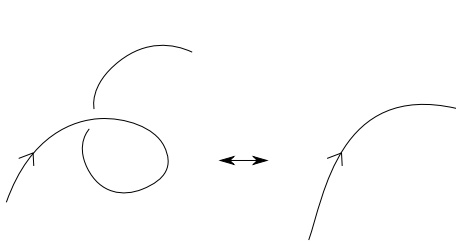


Figure 1: Removing a writhing (self-crossing of a link).

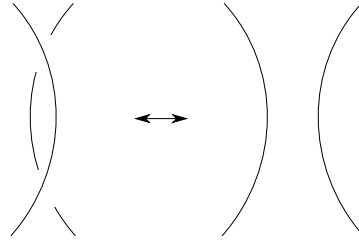


Figure 2: Sliding two links across one another.

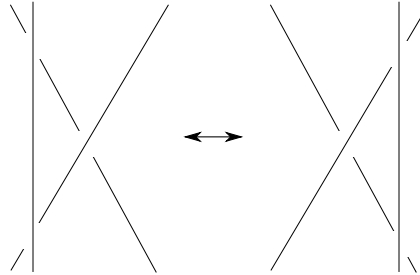


Figure 3: Sliding links under / over crossings.

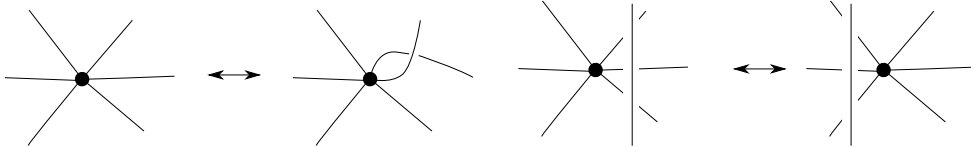


Figure 4: Twisting links at nodes. This changes the cyclic ordering of links.

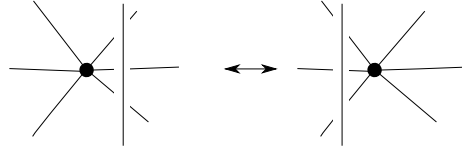


Figure 5: Sliding links under / over nodes.

Here $*$: $\wedge^4 \mathbb{R}^4 \rightarrow \mathbb{R}$ is the Hodge dual, and ℓ_1 and ℓ_2 are the two edges participating at the crossing C . Since for bivectors B, B' , one has that $B \wedge B' = B' \wedge B$, it is not important which of the ℓ_1, ℓ_2 is the upper or lower link. The sum ranges over all crossings of the projection $\tilde{\Gamma}$.

The notation $I(\Gamma)$ instead of $I(\tilde{\Gamma})$ can be explained with the following proposition.

Proposition 2.1. *The number $I(\Gamma)$ is invariant under the moves described above.*

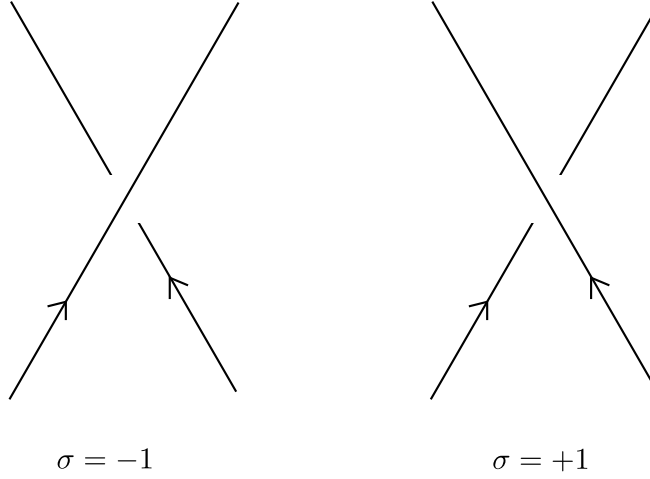


Figure 6: The two possible knotting cases, which get assigned $\sigma = -1$ and $\sigma = +1$, respectively. Note how in both cases there is a well-defined *upper* and *lower* link.

Proof: a) follows directly from $B_\ell \wedge B_\ell = 0$, while b) follows from the fact that in any pair of over- or undercrossings C_1 and C_2 , the two generated crossings are of opposite type, i.e. $\sigma(C_1) = -\sigma(C_2)$, while the participating bivectors are the same in both crossings. c) follows from (2.3), while d) follows from (2.2) for $\ell \neq \ell'$. \square

Indeed, the number $I(\Gamma)$ only depends on the graph embedded in S^3 (up to ambient isotopy) and its bivector colouring, not on any choice of projection onto the plane with crossings.

Definition 2.3. Let Γ, Γ' be two bivector-coloured graphs embedded in S^3 . Denote $\Gamma \sim \Gamma'$, if one arises from the other by a finite sequence of the following moves (or their inverses):

1. A continuous ambient isotopy, i.e. a homeomorphism of S^3 to itself,
2. A change of orientation of a link ℓ , accompanied by a change of $B_\ell \rightarrow -B_\ell$,
3. In case that there are two nodes v_1 and v_2 , and a link $\ell \supset v_{1,2}$ between them, such that all pairs of bivectors $B_\ell, B_{\ell'}$ for links touching either of the two nodes satisfy $B_\ell \wedge B_{\ell'} = 0$: A merging of the two nodes, i.e. remove both $v_{1,2}$ and link ℓ , and replace it with another node v in their vicinity, with all other links connected to v (see figure 7).
4. In case that there are two nodes v_1, v_2 and two similarly-oriented links $\ell_{1,2} \supset v_{1,2}$, such that there is an ambient isotopy which moves ℓ_1 to ℓ_2 , but leaves all $\ell \neq$

$\ell_{1,2}$ untouched: A merging of those two links, i.e. remove ℓ_2 , and replace B_{ℓ_1} by $B_{\ell_1} + B_{\ell_2}$ (see figure 8).

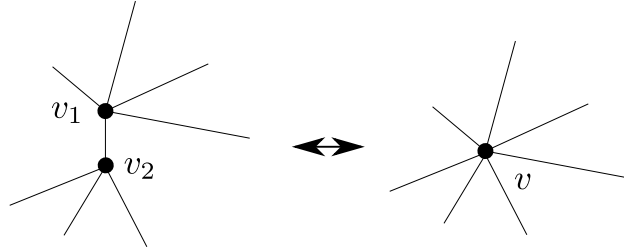


Figure 7: The merging of two nodes v_1, v_2 to v is only allowed, if all links meeting at either v_i satisfy (2.2).

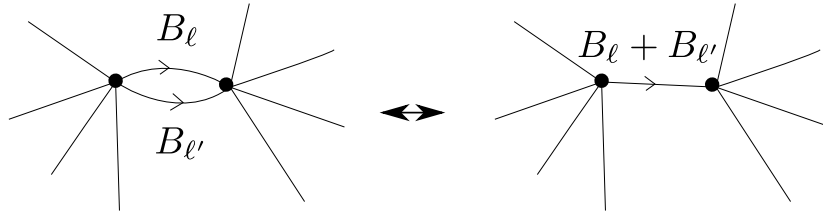


Figure 8: The merging of two links is always allowed.

Proposition 2.2. *The moves prescribed in definition 2.3 transform simple bivector-coloured graphs to simple bivector-coloured graphs.*

Proof: It is straightforward to show that neither 1.), 2.) nor 4.) change (2.2) or (2.3). It is also clear that after a merging of nodes the new node satisfies (2.3), since the removed link was ingoing into one, and outgoing of the other original node. By the condition, after the merging of nodes, the condition (2.2) holds for all new links at the new node, so 3.) also generates a simple bivector-coloured graph.

Proposition 2.3. *Let $\Gamma \sim \Gamma'$ be two bivector-coloured graphs, then $I(\Gamma) = I(\Gamma')$.*

Proof: By proposition 2.1, 1.) is clear. 3.) is also clear, since in any projection, we can make moves (fig. 1 – fig. 5), until ℓ does not partake in any crossing. If the conditions for 4.) are satisfied, one can find a projection such that neither ℓ_1 nor ℓ_2 partake in a crossing, so 4.) is true as well. To show invariance under 2.), just note that for any

crossing C between two different links, changing orientation of one of the links ℓ changes the sign of $\sigma(C)$. The accompanying sign change of B_ℓ compensates for it, so $I(\Gamma)$ is unchanged. \square

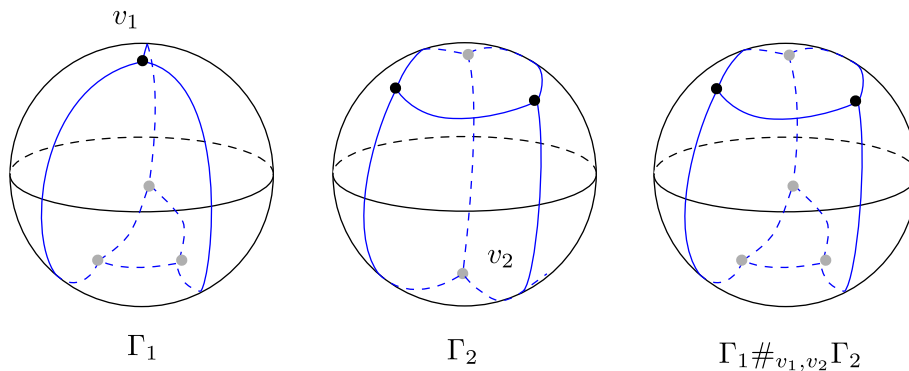


Figure 9: Two graphs Γ_1 and Γ_2 can be glued along two nodes, if the bivectors around those nodes agree and the link orientations are opposite. Figure shows the 3d analogue of the 4d procedure.

Definition 2.4. Consider two bivector-coloured graphs Γ_i , $i = 1, 2$. Assume that there are two nodes $v_i \in N(\Gamma_i)$, $i = 1, 2$, which have the following property: Around both, respectively exist open, simply-connected neighbourhoods $U_i \subset S^3$ containing v_i as the only node, and homeomorphisms ϕ_i in S^3 which map U_i to the northern (for $i = 1$) and southern (for $i = 2$) hemisphere of S^3 . Furthermore, let ϕ_i map ∂U_i to the equator $S^2 \subset S^3$, and v_i onto the north pole ($i = 1$) and south pole ($i = 2$), and the respective link segments onto geodesic lines from the respective pole to the equator (see figure 9).

Finally assume there is a one-to-one correspondence between links $\ell \supset v_1$ and links $\ell' \supset v_2$ such that

- To every link $\ell \supset v_1$ corresponds an $\ell' \supset v_2$ with $[v_1, \ell] = -[v_2, \ell']$.
- For every two such corresponding link pairs one has $B_\ell = B_{\ell'}$.
- For every such pair $\phi_1(\ell \cap \partial U_1) = \phi_2(\ell' \cap \partial U_2)$ is a point lying in S^2 .

If these conditions are satisfied, we say that Γ_1 and Γ_2 can be glued together (at v_1 and v_2). In that case, we can define a new bivector-coloured graph, denoted by $\Gamma_1 \#_{v_1, v_2} \Gamma_2$, which is such that

$$\begin{aligned} (\Gamma_1 \#_{v_1, v_2} \Gamma_2) \cap N &= \phi_1(\Gamma_1) \cap N, \\ (\Gamma_1 \#_{v_1, v_2} \Gamma_2) \cap S &= \phi_2(\Gamma_2) \cap S, \end{aligned}$$

where N, S , are the northern and southern hemisphere of S^3 , respectively.

Figure 9 shows a 3-dimensional analogue the construction. In essence, two bivector-coloured graphs which have “opposite nodes”, i.e. which have two nodes with the same incident links and bivectors on those links, but negative relative orientation, can be “glued together” along those two nodes. If both Γ_i , $i = 1, 2$ are simple, then so is $\Gamma_1 \#_{v_1, v_2} \Gamma_2$, of course.

The concept is analogous to the well-known procedure of surgery from differential geometry. However, the condition on the two nodes is quite severe, and it may well be that two graphs cannot be glued together like this at all.

Proposition 2.4. *For any two simple bivector-coloured graphs Γ_1 and Γ_2 which can be glued along v_1 and v_2 , one has*

$$I(\Gamma_1 \#_{v_1, v_2} \Gamma_2) = I(\Gamma_1) + I(\Gamma_2). \quad (2.5)$$

Proof: One can find (by using ambient isotopies, or projecting from points close to the north pole) projections such that $\phi_1(\Gamma_1 \cap U_1)$ is being projected to $\mathbb{R}^2 \setminus D$ (where D is the solid circle with radius 1), with no crossings inside D . Also, $\phi_2(\Gamma_2 \cap U_2)$ can be mapped to D , where the only crossings outside of D are among bivectors B_1, B_2 with $B_1 \wedge B_2 = 0$, due to simplicity. The claim then follows due to the additivity of (2.4) as sum over crossings.

3 Convex polytopes in $d = 4$.

Convex polytopes P in \mathbb{R}^4 can be represented via a set of half-spaces $H_i = \{x \in \mathbb{R}^4 : \langle x, u_i \rangle \leq 1\}$, with $u_i \in \mathbb{R}^4$, via

$$P = \bigcap_{i=1}^n H_i. \quad (3.1)$$

We assume that the presentation is irreducible, i.e. none of the H_i can be removed without changing P . In this case, there is a one-to-one correspondence between half-spaces H_i and 3-dimensional faces

$$\tau_i = P \cap \partial H_i. \quad (3.2)$$

Each of the 3-faces τ_i itself is a convex 3-dimensional polytope lying in the 3-dimensional affine subspace ∂H_i . Two neighbouring 3-faces can touch at a common 2-face f , in which case

$$f = \tau_i \cap \tau_j = P \cap \partial H_i \partial H_j \quad (3.3)$$

is a convex 2-dimensional polygon.

Definition 3.1. The (boundary) graph Γ_P of a 4-polytope P is a graph embedded in S^3 , defined the following way: Without loss of generality, let the origin of \mathbb{R}^4 lie inside of P . Consider the sphere S^3 with radius 1, and project every point on $\partial P = \cup_i \tau_i$ onto S^3 , via

$$\pi : \partial P \rightarrow S^3, \quad \pi(x) \rightarrow \frac{x}{|x|}. \quad (3.4)$$

Choose a point v_i in each $\pi(\tau_i)$. These are the nodes of Γ_P . For two neighbouring τ_i , connect the corresponding v_i with a geodesic arc in S^3 , such that it passes through $\pi(f)$. These are the links ℓ of Γ_P .

The thus constructed graph is, of course, not unique. But different choices are equivalent under homeomorphisms of S^3 . Note that each link ℓ in Γ_P is in one-to-one correspondence with 2-faces f in P . Also note that Γ_P does not come with an orientation for its links, but a choice of such is equivalent to an orientation of the corresponding f in the following way: Each orientation of $f \subset P$ is given by a non-vanishing 2-form ω_f , which can be pulled back to a 2-form defined on $\pi(f) \subset S^3$. Using the standard metric on S^3 , we can convert this via musical isomorphism and Hodge duality to a non-vanishing normal vector field X on $\pi(f)$. Then orient ℓ such that X points from the source 3-polytope of ℓ to its target 3-polytope (see figure 10).

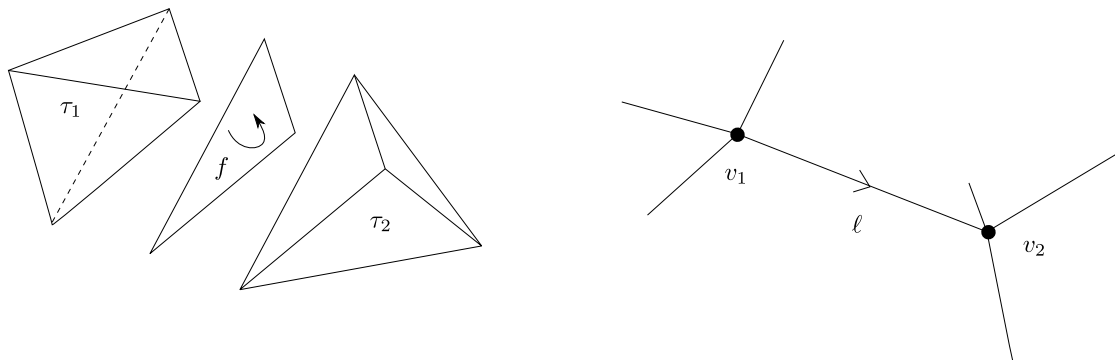


Figure 10: An orientation of a face f in P determines the orientation of the link ℓ dual to it in Γ_P , and vice versa.

Definition 3.2. For a 2-face $f \subset P$, and a chosen orientation ω_f on it, define the (unique) bivector

$$B_f := N \wedge M, \quad (3.5)$$

where $N, M \in \mathbb{R}^4$ are vectors that span f , such that $\omega_f(B_f) > 0$ and $|B_f| = |N||M| \sin \theta$, where θ is the angle between N and M . For a given choice of orientation of all faces, this defines an orientation of links of Γ_P , and, due to the one-to-one correspondence of faces f and links ℓ , a bivector-colouring of Γ_P . This is also called the bivector geometry of P .

Proposition 3.1. *For a convex 4-polytope, the bivector geometry is a simple bivector-colouring of Γ_P .*

Proof: The simplicity condition (2.2) follows from the fact that, for two faces $f_{1,2} \subset \tau$, the bivectors satisfy $B_{f_1} \sim N_1 \wedge M_1$, and $B_{f_2} \sim N_2 \wedge M_2$. But all four vectors $N_{1,2}, M_{1,2}$ lie in the $3d$ subspace parallel to the $3d$ polyhedron τ , hence they are linearly dependent. Thus $B_{f_1} \wedge B_{f_2} \sim N_1 \wedge M_1 \wedge N_2 \wedge M_2 = 0$.

To prove the closure condition (2.3), we consider w.l.o.g. the case that all links are outgoing of n . Denote the area of f by a_f , and choose N_f and M_f as two orthogonal normalized vectors lying in the plane parallel to the face f , such that $B_f = a_f N_f \wedge M_f$ for all $f \subset \tau$. Denote by T the normalized vector orthogonal to τ , and for each f let O_f be the normalized vector in the $3d$ space parallel to τ orthogonal to N_f and M_f , such that (T, N_f, M_f, O_f) is positively oriented. Minkowski's theorem [37] states that

$$\sum_{f \subset \tau} a_f O_f = 0. \quad (3.6)$$

Since $*(T \wedge O_f) = N_f \wedge M_f$, the claim follows. \square

Proposition 3.2. *Let P be a 4-polytope, and $H \subset \mathbb{R}^4$ a half-space such that $P_1 := H \cap P$, $P_2 := (-H) \cap P$ are two 4-polytopes. Here $(-H) := \overline{\mathbb{R}^4} \setminus \overline{H}$. If v_1 is the node of Γ_{P_1} corresponding to the 3-face $\partial H \cap P_1$, and v_2 the node corresponding to the 3-face $\partial(-H) \cap P_2$, then*

$$\Gamma_{P_1} \#_{v_1, v_2} \Gamma_{P_2} \sim \Gamma_P. \quad (3.7)$$

Proof: First we characterise the boundary graphs $\Gamma_{1,2}$. The polytope P has a representation as intersection of half-spaces as

$$P = H_1 \cap H_2 \cap \cdots \cap H_n. \quad (3.8)$$

Corresponding to these, we numerate the 3-faces of P as $\tau_i = \partial H_1 \cap P$. Intersecting this with H and $(-H)$, respectively, one can w.l.o.g. find an irreducible representation in terms of

$$\begin{aligned} P_1 &= H \cap H_1 \cap \cdots \cap H_k \cap H_{k+1} \cap \cdots \cap H_m, \\ P_2 &= (-H) \cap H_1 \cap \cdots \cap H_k \cap H_{m+1} \cap \cdots \cap H_n, \end{aligned}$$

with $k \leq m \leq m$. Note that it is possible that $k = m$, but not that $m = n$. The boundary 3-faces τ_1, \dots, τ_k of P are therefore the ones which get separated into two 3-faces by ∂H , and thus also appear in both P_1 and P_2 . W.l.o.g. we assume that the half-space H is $H = \{x \in \mathbb{R}^4 \mid x^1 \geq 0\}$, i.e. $(-H) = \{x \in \mathbb{R}^4 \mid x^1 \leq 0\}$. Furthermore, for τ_i and τ_j sharing a common face f with $k < i \leq m$ and $m < j \leq n$, that face f has a corresponding link ℓ which connects a node in the northern and southern hemisphere, i.e. crosses the equator $E \simeq S^2 \subset S^3$. We furthermore assume w.l.o.g. that each node corresponding to a 3-face τ_i , $1 \leq i \leq k$, lies on E , as well as any link between two such neighbouring nodes.

The 3-face $\tau = \partial H \cap P_1$ in P_1 has as 2-faces those which are on the boundary of τ , i.e. those which are either intersections of $\tau_i \cap \partial H$, with $1 \leq i \leq k$, or those which are faces between τ_i and τ_j , with $k < i \leq m$, $m < j \leq n$.

Now the construction of Γ_{P_1} can be achieved as follows: Consider $\Gamma \cap H$, which gives a graph (with open ends) on the northern hemisphere of S^3 . Add to this another node p at the south pole (corresponding to the 3-face $\tau_p = \partial H \cap P_1$), and connect it to those nodes which lie on the equator E . Also, extend every link which passed from the northern to the southern hemisphere (and which now ends on the equator) to the south pole. Then the new links (those from the equator to the south pole) are equipped with an orientation, and the corresponding B_f . Denote the nodes of P_1 , which correspond to H_1, \dots, H_k , by w_1, \dots, w_k , while the nodes v_{k+1}, \dots, v_m are identical to those of P .

The construction of Γ_{P_2} runs along the same lines, where the new node q , corresponding to the new 3-face $\tau_q = \partial(-H) \cap P_2$, is placed on the north pole, and all new orientations of faces are chosen to be opposite to the corresponding ones in P_1 (see figure 11). Denote the nodes of P_2 which correspond to H_1, \dots, H_k by x_1, \dots, x_k , while those corresponding to H_{m+1}, \dots, H_n , which are identical to those of P , as v_{m+1}, \dots, v_n .

With these conventions, it is clear that $\Gamma_{P_1} \#_{p,q} \Gamma_{P_2}$ can be constructed. However, it is not the same as the original Γ . The reason is that in $\Gamma_{P_1} \#_{p,q} \Gamma_{P_2}$, every node which corresponds to τ_i , $1 \leq i \leq k$, appears twice, as does every link between two such nodes. The reason is that, after glueing the pieces P_1 and P_2 back together, the resulting polytope is not quite P , but P where every 3-face τ_1, \dots, τ_k has been trivially subdivided, so that it counts as two distinct 3-faces.

In particular, the graph $\Gamma_{P_1} \#_{p,q} \Gamma_{P_2}$ does not contain the nodes v_1, \dots, v_n , but rather $w_1, \dots, w_k, x_1, \dots, x_k, v_{k+1}, \dots, v_n$. Each w_i is connected to x_i for $1 \leq i \leq k$. Since the associated 3-faces are the result of cutting a 3-face (dual to v_i in Γ) into two, the bivectors of both w_i and x_i lie in the same affine $3d$ -subspace which contains τ_i . Hence, the conditions for the move in figure 7 are satisfied, and we can merge the two nodes to a v_i . If there is a link ℓ between w_i and w_j , then there is of course also one ℓ' between x_i and x_j . Hence, after merging the nodes, we have two links from v_i to v_j . These can be merged to one link, and since the bivectors B_ℓ and $B_{\ell'}$ are the area bivectors of a face f cut in two, we have $B_\ell + B_{\ell'} = B_f$. Hence, after merging the nodes and links which

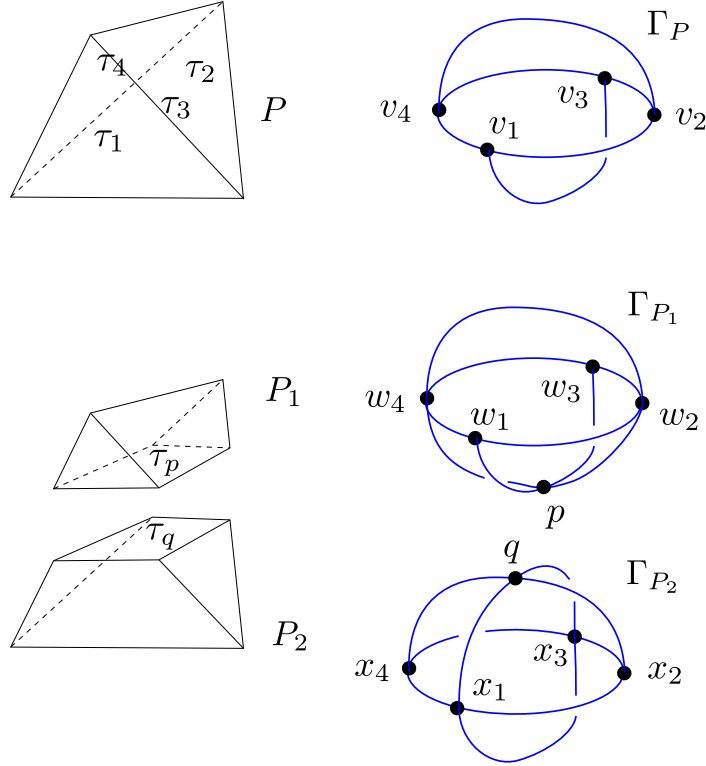


Figure 11: Subdivision of a polyhedron P into two P_1 and P_2 , by cutting with a hyperplane. The corresponding boundary graphs get changed correspondingly. This is a $3d$ representation of the $4d$ construction. All four faces of P are subdivided, so in the boundary graph, all four nodes lie on the equator (and get doubled in the cutting process). The new links connecting these four to v_1 and v_2 , respectively, have opposite orientation (not depicted).

were originally on E , we are back to the original graph Γ . □

Corollary 3.1. *Let P be a 4-dimensional convex polytope, embedded in \mathbb{R}^4 . Let H be a 3d half-space which cuts P into two convex 4d polytopes P_1 and P_2 . Then*

$$I(\Gamma_P) = I(\Gamma_{P_1}) + I(\Gamma_{P_2}). \quad (3.9)$$

Proof: This follows immediately from propositions 2.3, 2.4 and 3.2. □

This means that I associates, to every convex 4d polytope, a number in such a way that it is additive under gluing of two convex polytopes to one. The following proposition

elucidates the meaning of this number.

Proposition 3.3. *Let P be a 4-simplex. Then $I(\Gamma_P) = V_P$, where V_P is the 4-volume of P .*

Proof: This can be shown easily by realizing that there is a projection of Γ_P onto the plane with only one crossing (see figure 12).

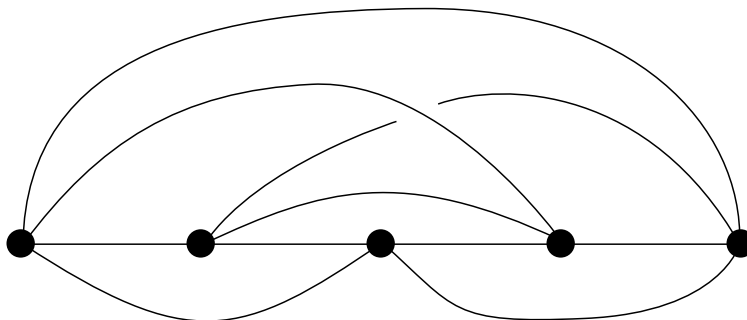


Figure 12: The boundary graph of a 4-simplex.

Each boundary 3-face of P is a tetrahedron, which is the convex hull of all but one vertex of P . We label the nodes in Γ_P in figure 12 N_1, \dots, N_5 from left to right, and decree that N_i is the tetrahedron spanned by all vertices but the i -th one.

The 2-faces of P are triangles, which are spanned by three vertices in P . From the figure, one can easily see that the crossing takes place between the triangles $f_1 = (235)$ and $f_2 = (134)$. Denoting 1-faces by (ij) if the corresponding 4-vectors $e_{(ij)}$ going from i to j , we can see that (given an orientation of edges such that $\sigma(C) = +1$)

$$B_{f_1} = \frac{1}{2}e_{(35)} \wedge e_{(32)}, \quad B_{f_2} = \frac{1}{2}e_{(31)} \wedge e_{(34)}. \quad (3.10)$$

All of these vectors start at vertex 3, and they span P . In particular, from basic geometry, the formula for the 4-volume of a 4-simplex is given by

$$V = \frac{1}{24} * (e_{(35)} \wedge e_{(32)} \wedge e_{(31)} \wedge e_{(34)}). \quad (3.11)$$

The claim follows. □

In other words, the number I associates (up to a factor) the 4-volume to a 4-simplex. So, whenever I associates the volume to two polytopes which can be glued together, I also associates the volume to the result of the glueing. Of course, every 4-dimensional

polytope can be built up from 4-simplices, but there is a subtle caveat we have to clarify, before we can conclude that I indeed associates the 4-volume to every 4-polytope. Namely, in the conditions of proposition 3.2, all three P_1 , P_2 , and P need to be convex. However, by successively building up a 4-polytope from 4-simplices, e.g. by a triangulation, generically intermediate steps will be non-convex. So, we need to show that every 4-polytope can be successively built up from smaller convex pieces, starting with 4-simplices, such that each intermediate step is also convex. This is what we will establish in what follows.

Definition 3.3. *Assume that, for some convex polytope $P \subset \mathbb{R}^d$, there is a sequence of collections of convex polytopes*

$$\{P_1^{(1)}\} \rightarrow \{P_1^{(2)}, P_2^{(2)}\} \rightarrow \{P_1^{(3)}, P_2^{(3)}, P_3^{(3)}\} \rightarrow \dots \rightarrow \{P_1^{(m)}, \dots, P_m^{(m)}\}, \quad (3.12)$$

such that for one $1 \leq m \leq k$ one has

$$P_l^{(k)} = P_l^{(k+1)} \cup P_{l+1}^{(k+1)}, \quad (3.13)$$

while $P_i^{(k)} = P_i^{(k+1)}$ for $i < l$, and $P_i^{(k)} = P_{i+1}^{(k+1)}$ for $i > l$. If all $P_i^{(m)}$, $i = 1, \dots, m$ are d -simplices, then we call P convex-divisible.

Proposition 3.4. *Every polytope in $d = 2$ is convex-divisible.*

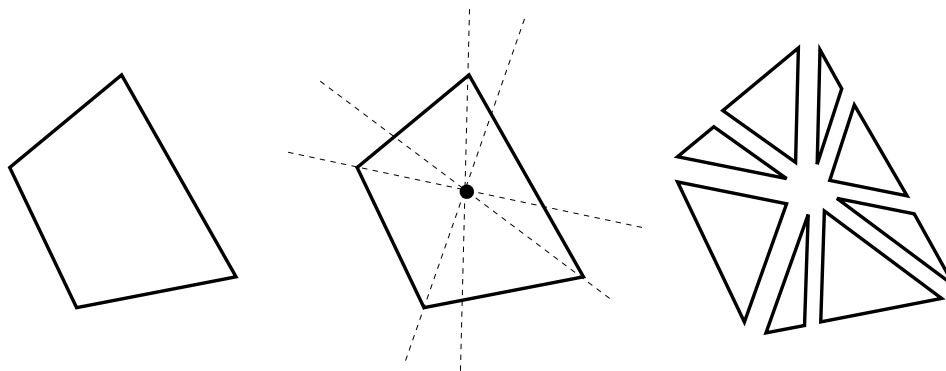


Figure 13: Subsequent subdivision of a $4d$ polytope, by the hyperplanes spanned by a vertex v and all $2d$ boundary faces f . This is a $2d$ representation of the $4d$ construction, where the boundary faces are 0-dimensional vertices.

Proof:

A polytope in $d = 2$ is a polygon with n vertices. Choose a cyclical numbering of these as v_1, v_2, \dots, v_n . If $n = 3$, one is done. If $n > 3$, then for the first step, cut

$P = P_1^{(1)}$ along the line connecting v_1 and v_3 . Then $P_1^{(2)}$ is the triangle with vertices v_1, v_2, v_3 , and $P_2^{(2)}$ is the remainder, which has one fewer vertex than P . Repeat this process, which stops after $n - 3$ steps. \square

Proposition 3.5. *Let P be a convex polytope in d dimensions. If every polytope in dimension $d - 1$ is convex-divisible, then P is convex-divisible.*

Proof: Choose a vertex v in P which is not on the boundary. Every $d - 2$ -face f of P is the intersection of two boundary $d - 1$ -polytopes τ_1 and τ_2 in P . The vertices of f lie completely in the $d - 1$ -dimensional hyperplane spanned by e.g. τ_1 . Since v does not lie in that plane, by construction, v and the vertices of f span a $d - 1$ -dimensional hyperplane which separates P into two, such that τ_1 and τ_2 lie on either side.

Let there be N $d - 2$ -faces in P , then the N hyperplanes H_f spanned by f and v successively split the polytope P into $M \leq 2^N$ sub-polytopes $P_i^{(m)}$, $i = 1, \dots, m$. Each of these $P_i^{(m)}$ contains v as a vertex. Every $P_i^{(m)}$ also contains at least one inner point of one of the $d - 1$ -dimensional boundary faces τ . By construction, $P_i^{(m)}$ then cannot contain any inner point of a different $d - 1$ face $\tau' \neq \tau$, since in P these two are separated by at least one H_f .

Hence, each of the $P_i^{(m)}$ is a sub-polytope of the pyramid with τ as base and v as tip. In fact, it can be generated from that by intersecting this pyramid with half-spaces having v on its boundary. As a result, each $P_i^{(m)}$ is a pyramid which has v on its tip, and a convex sub-polytope $\hat{\tau} \subset \tau$ as its base.

By our initial condition, $\hat{\tau}$ is convex-divisible, since it is a convex $d - 1$ -dimensional polytope. The series of its subdivision determines a subdivision of each $P_i^{(m)}$, by taking the pyramid with tip v (i.e. the suspension over v). The result is a series of d -dimensional polytopes being pyramids with bases $d - 1$ -simplices, and tip v . Of course, each of those is a d -simplex, so as soon as we have chosen an order of subsequent subdivision of the $P_i^{(m)}$, we are done.

Corollary 3.2. *Every convex polytope in any dimension $d \geq 2$ is convex-divisible.*

With this, we finally have everything we need to prove the central claim of this article.

Lemma 3.1. *For any convex 4-polytope P , we have that*

$$I(\Gamma_P) = V_P, \tag{3.14}$$

where V_P is the 4-volume of P .

Proof: By corollary 3.2, we can choose a subsequent subdivision of P into convex sub-polytopes, until we arrive a collection of 4-simplices. By using propositions 2.4 and 3.3, the claim follows. \square

4 Summary

In this article we have delivered a proof for the formula (1.1), which relates the volume V_P of a $4d$ polytope P with its $2d$ bivectors B_f , and the crossings C in its boundary graph. Besides its geometrical meaning, the quantization of this formula allows to add a cosmological constant term to the Euclidean signature EPRL-FK Spin Foam model, without resorting to quantum deforming the Hilbert spaces, which made the renormalization of the asymptotical formula accessible in a truncated setting [38, 39, 28]. Also, it allows for a formulation of the quadratic volume simplicity constraint, which is not properly imposed in the KKL extension of the EPRL-FK model [20, 23, 39]. Whether this constraint is sufficient to allow for geometric reconstruction of a $4d$ geometry from the boundary state is still open, and it appears that a linear version of the volume simplicity constraint might be suitable to achieve this [23].

The proof relied on the convexity of the polytope P . However, geometrically it seems feasible to assume that the formula is true even for non-convex polytopes, as long as the boundary is homeomorphic to S^3 , i.e. the polytope is simply-connected. In particular, formula (3.7), which prescribes the behaviour of the invariant under glueing, is certainly true also for non-convex polyhedra. The main technical difficulty lies in the exact definition of non-convex polytope, of which there are several inequivalent ones, and a mathematical description which does not rely on the intersection of half-spaces, which only works for the convex case.

This might be of interest, since non-convex polytopes also appear in the asymptotic analysis of the EPRL-FK model, if $3d$ boundary data admits non-convex glueing in $4d$. The question remains whether these should be suppressed in the path integral or not. A version of the volume simplicity constraint (in particular a linear one, which amounts to $4d$ -closure of $3d$ normals) might help in this regard. We aim at returning to this point in another publication.

Acknowledgements

The author is indebted to John Barrett and Nathan Bowler for helpful discussions. This work was funded by the project BA 4966/1-1 of the German Research Foundation (DFG).

References

- [1] T. Thiemann, *Modern Canonical Quantum General Relativity*. Cambridge: Cambridge University Press, 2008.
- [2] C. Rovelli, *Quantum gravity*. Cambridge: Cambridge University Press, 2004.

- [3] A. Perez, “The Spin Foam Approach to Quantum Gravity,” *Living Rev. Rel.*, vol. 16, p. 3, 2013.
- [4] C. Rovelli and F. Vidotto, *Covariant Loop Quantum Gravity*. Cambridge Monographs on Mathematical Physics, Cambridge University Press, 2014.
- [5] J. Ambjorn, A. Gorlich, J. Jurkiewicz, and R. Loll, “Causal dynamical triangulations and the search for a theory of quantum gravity,” *Int. J. Mod. Phys.*, vol. D22, p. 1330019, 2013.
- [6] L. Bombelli, J. Lee, D. Meyer, and R. Sorkin, “Space-Time as a Causal Set,” *Phys. Rev. Lett.*, vol. 59, pp. 521–524, 1987.
- [7] D. Oriti, “Group field theory as the microscopic description of the quantum space-time fluid: A New perspective on the continuum in quantum gravity,” *PoS*, vol. QG-PH, p. 030, 2007.
- [8] J. F. Plebanski, “On the separation of Einsteinian substructures,” *J. Math. Phys.*, vol. 18, pp. 2511–2520, 1977.
- [9] G. T. Horowitz, “Exactly Soluble Diffeomorphism Invariant Theories,” *Commun. Math. Phys.*, vol. 125, p. 417, 1989.
- [10] M. P. Reisenberger and C. Rovelli, “‘Sum over surfaces’ form of loop quantum gravity,” *Phys. Rev.*, vol. D56, pp. 3490–3508, 1997.
- [11] J. C. Baez, “An Introduction to spin foam models of quantum gravity and BF theory,” *Lect. Notes Phys.*, vol. 543, pp. 25–94, 2000.
- [12] J. W. Barrett, R. J. Dowdall, W. J. Fairbairn, H. Gomes, and F. Hellmann, “Asymptotic analysis of the EPRL four-simplex amplitude,” *J. Math. Phys.*, vol. 50, p. 112504, 2009.
- [13] J. W. Barrett, R. J. Dowdall, W. J. Fairbairn, F. Hellmann, and R. Pereira, “Lorentzian spin foam amplitudes: Graphical calculus and asymptotics,” *Class. Quant. Grav.*, vol. 27, p. 165009, 2010.
- [14] F. Conrady and L. Freidel, “On the semiclassical limit of 4d spin foam models,” *Phys. Rev.*, vol. D78, p. 104023, 2008.
- [15] J. W. Barrett and L. Crane, “Relativistic spin networks and quantum gravity,” *J. Math. Phys.*, vol. 39, pp. 3296–3302, 1998.
- [16] J. Engle, E. Livine, R. Pereira, and C. Rovelli, “LQG vertex with finite Immirzi parameter,” *Nucl. Phys.*, vol. B799, pp. 136–149, 2008.

- [17] L. Freidel and K. Krasnov, “A New Spin Foam Model for 4d Gravity,” *Class. Quant. Grav.*, vol. 25, p. 125018, 2008.
- [18] A. Baratin, C. Flori, and T. Thiemann, “The Holst Spin Foam Model via Cubulations,” *New J. Phys.*, vol. 14, p. 103054, 2012.
- [19] A. Baratin and D. Oriti, “Group field theory and simplicial gravity path integrals: A model for Holst-Plebanski gravity,” *Phys. Rev.*, vol. D85, p. 044003, 2012.
- [20] W. Kaminski, M. Kisielowski, and J. Lewandowski, “Spin-Foams for All Loop Quantum Gravity,” *Class. Quant. Grav.*, vol. 27, p. 095006, 2010. [Erratum: *Class. Quant. Grav.*29,049502(2012)].
- [21] B. Bahr and S. Steinhaus, “Investigation of the Spinfoam Path integral with Quantum Cuboid Intertwiners,” *Phys. Rev.*, vol. D93, no. 10, p. 104029, 2016.
- [22] B. Bahr and V. Belov, “On the volume simplicity constraint in the EPRL spin foam model,” 2017.
- [23] V. Belov, “Poincaré-Plebański formulation of GR and dual simplicity constraints,” 2017.
- [24] B. Dittrich and S. Speziale, “Area-angle variables for general relativity,” *New J. Phys.*, vol. 10, p. 083006, 2008.
- [25] L. Freidel and S. Speziale, “Twisted geometries: A geometric parametrisation of $SU(2)$ phase space,” *Phys. Rev.*, vol. D82, p. 084040, 2010.
- [26] L. Freidel and J. Ziprick, “Spinning geometry = Twisted geometry,” *Class. Quant. Grav.*, vol. 31, no. 4, p. 045007, 2014.
- [27] B. Bahr and G. Rabuffo, “Deformation of the EPRL spin foam model by a cosmological constant,” 2018.
- [28] B. Bahr, G. Rabuffo, and S. Steinhaus, “Renormalization in symmetry restricted spin foam models with curvature,” 2018.
- [29] M. Han, “Cosmological Constant in LQG Vertex Amplitude,” *Phys. Rev.*, vol. D84, p. 064010, 2011.
- [30] H. M. Haggard, M. Han, W. Kaminski, and A. Riello, “ $SL(2, \mathbb{C})$ Chern-Simons Theory, a non-Planar Graph Operator, and 4D Loop Quantum Gravity with a Cosmological Constant: Semiclassical Geometry,” *Nucl. Phys.*, vol. B900, pp. 1–79, 2015.

- [31] W. J. Fairbairn and C. Meusburger, “Quantum deformation of two four-dimensional spin foam models,” *J. Math. Phys.*, vol. 53, p. 022501, 2012.
- [32] M. Han, “4-dimensional Spin-foam Model with Quantum Lorentz Group,” *J. Math. Phys.*, vol. 52, p. 072501, 2011.
- [33] B. Dittrich and M. Geiller, “Quantum gravity kinematics from extended TQFTs,” 2016.
- [34] K. Reidemeister, “Elementare Begründung der Knotentheorie,” *K. Abh. Math. Semin. Univ. Hambg.*, vol. 4, 1927.
- [35] J. W. Alexander and G. B. Briggs, “On types of knotted curves,” *Ann. of Math.*, vol. 2, 1926.
- [36] J. L. Gross and T. W. Tucker, *Topological Graph Theory*. Wiley Interscience, 1987.
- [37] H. Minkowski, “Allgemeine Lehrsätze ueber die convexen Polyeder,” *Nachrichten v. d. Gesellschaft d. Wissenschaften zu Goettingen*, 1897.
- [38] B. Bahr and S. Steinhaus, “Numerical evidence for a phase transition in 4d spin foam quantum gravity,” *Phys. Rev. Lett.*, vol. 117, no. 14, p. 141302, 2016.
- [39] B. Bahr and S. Steinhaus, “Hypercuboidal renormalization in spin foam quantum gravity,” *Phys. Rev.*, vol. D95, no. 12, p. 126006, 2017.